J. Coat. Technol. Res., **19** (2) 607–616, 2022
https://doi.org/10.1007/s11998-021-00550-5

Modification of styrene-acrylic emulsion by organic UV absorber in synergy with fluorine and silicon monomers for weatherable coatings

Wei Dong, Lei Zhou, Yanni Guo, Yining Tang, Rong Pan, Mengli Liu, Deliang He

Received: 8 June 2021 / Revised: 18 August 2021 / Accepted: 19 August 2021

Abstract To improve the weather ability and thermal stability of styrene-acrylic polymer emulsion coatings, a series of novel styrene-acrylic polymer emulsion modified with 2-[2-hydroxy-5-[2-(methacryloyloxy)ethyl]phenyl]-2H-benzotriazole (HMEB), hexafluorobutyl methacrylate (HFMA), and vinyltrimethoxysilane (VTMS) were prepared through semi-continuous seed emulsion polymerization. The emulsions and their coatings were characterized by Fourier transform infrared spectroscopy, ultraviolet absorption spectroscopy (UV-Vis), X-ray photoelectron spectroscopy, dynamic laser scattering, transmission electron microscopy, zeta potential, thermogravimetric analysis, and artificially accelerated aging test. According to the results, the new polymer emulsion had superior UV absorption from 308 to 364 nm. Moreover, the coating performed the best anti-aging stability when the content of HMEB, HFMA, and VTMS reached 4%, 2%, and 3%, respectively. After the 1000 h aging test, the color difference (ΔE) and rate of loss of gloss (ΔG) were only 6.86% and 51.10%, while the unmodified coatings were 16.05% and 72.22%, respectively. Furthermore, the thermal stability and water resistance of the coating were improved by fluorine and silicon monomers. The initial decomposition temperature was increased from 327 to 339°C. Moreover, the UV stabilization mechanism is preliminarily discussed.

Keywords Benzotriazole, Styrene-acrylic polymer emulsion, UV absorption, Weather resistance, Silicon-fluorinated

W. Dong, L. Zhou, Y. Guo, Y. Tang, R. Pan, M. Liu, D. He (✉)
College of Chemistry and Chemical Engineering, Hunan University, Changsha 410082, China
e-mail: delianghe@hnu.edu.cn

Introduction

Styrene-acrylic polymer emulsion, widely applied in various building fields, is composed of acrylate and styrene monomers with good physical and mechanical properties, good environmental protection performance, and low price. However, the emulsion polymer is a linear structure, so the water resistance,[1] heat resistance,[2] stain resistance,[3] and weather resistance[4, 5] of the prepared coatings are not excellent, causing problems when used as outdoors coatings. Therefore, the high-performance synthesis of novel styrene-acrylic polymer emulsions has become one of the hot spots in construction.[6–8]

Organic coatings in outdoor applications are vulnerable to ultraviolet (UV) damage, including gloss loss, color difference, powder, cracking.[9–13] Improving the weather resistance of the coating is the key to solve these problems. In general, to improve the weather resistance of organic coatings, the modification of film-forming resin and nano-modification can be considered to reduce UV light damage. Some nanoparticles have super absorption or scattering properties to UV light and are used to slow down the aging process of coatings. For example, $FeTiO_3$, CeO_2, TiO_2, ZnO, and other nanoparticles reduce the action strength caused by UV light to a certain extent.[14–21] However, although nanomaterials improve the UV resistance of the coatings, their stability, dispersion, compatibility with the coatings, high price, and influence on the light transmittance of the transparent substrate are still challenging, especially for human health and the environment. On the other hand, in the presence of reactive oxygen species and humidity, nanoparticles are used as photocatalysts to accelerate the degradation of coatings.[15,22,23]

UV absorbers, such as benzotriazole, aromatic ester, and tannin additive,[24,25] are used in coatings because they selectively and strongly protect polymers by

absorbing UV light and converting it into harmless low-energy radiation. However, the benzophenone UV absorber is not very photostable.[26] Aromatic ester UV absorbers have poor photostability and short absorption wavelength, so they need to be used with other UV absorbers.[27] Benzotriazole UV absorber is an environmentally friendly UV absorber that effectively absorbs 300–400 nm UV light and almost no visible light, with low toxicity and good stability. Rao et al.[18] compared the effects of benzotriazole-type UV (BTZ) and inorganic nano-ZnO UV absorbers on the weatherability of acrylate polymers. After 500 h of artificial UV lamp accelerated aging, BTZ improved the photooxidation resistance of acrylate coatings. Li et al.[10] dispersed 2-(2-hydroxy-3-tert-butyl-5-methylphenyl)-5-chlorinated benzotriazole in the coating and improved the UV radiation resistance of the coating. However, the physically mixed UV absorbers have disadvantages, including low binding force, easy migration, and volatilization, which cannot keep long-term protection in the coating. Therefore, if reactive UV stabilizers were bonded into the polymer by chemical reaction, the abovementioned problems could be effectively solved.[28] Moreover, if fluorine monomers and silicone monomers with good thermal stability and weathering resistance are incorporated into the polymers together with UV stabilizers, unexpected modification effects will be produced.[1,7,29–31] Currently, some reports on the modification of polymers by UV absorbers are available, but there are few reports on the modification of styrene-acrylic emulsions by UV absorbers combined with organic fluorine and silicone.

In this study, a series of novel UV-absorbing silicon-fluorinated styrene-acrylic emulsions were successfully prepared through semi-continuous seed emulsion polymerization. As a UV absorber, 2-[2-hydroxy-5-[2-(methacryloyloxy) ethyl] phenyl]-2H-benzotriazole (HMEB) contains acrylyl reactive groups, which can be copolymerized with acrylate monomer emulsions to give the coating a long-term practical UV resistance compared to physical blending. TEM, FTIR, UV-Vis, XPS, DLS, zeta potential, TGA, and fluorescence UV lamp accelerated aging test characterized the emulsions and coatings. Furthermore, to verify the UV protection value of weather resistance coatings, the best weather resistant coating was selected as UV shields for organic thermochromic microcapsules to investigate the chromatic variance of organic thermochromic materials.

Experimental

Materials

Ammonium persulfate (APS), sodium bicarbonate ($NaHCO_3$), triton X-100 (TX-100), sodium dodecylbenzene sulfonate (SDBS), methyl methacrylate (MMA), butyl acrylate (BA), styrene (St), hydroxyethyl methacrylate (HEMA), acrylic acid (AA), and ethylene glycol (EG) were purchased from Sinopharm Chemical Reagent Co., Ltd, China. Hexafluorobutyl methacrylate (HFMA), HMEB, and vinyl tri-methoxy silane (VTMS) were purchased from Guangdong Wengjiang Chemical Reagent Co., LTD. 3-allyloxygen-2-hydroxy-1-propane sulfonate sodium salt (COPS-1) was purchased from Shanghai Bi De Pharmaceutical Technology Co., LTD. Organic silicone resin WB300 is from Hunan Xiaohan Chemical Anticorrosion Co., LTD., China. Organic thermochromic material (65°C, blue) is from Shenzhen Jingyi Technology Co., LTD., China. DI water was made at the lab.

Pre-emulsification

Table 1 shows the preparation formula of the emulsion polymer. First, 26 g of DI-water and 70% emulsifier were added to the 250 mL beaker and stirred with a magnetic stirrer. All the monomers were weighted within 20 min and added in a drop-wise manner into the beaker using a dropping funnel. The monomers were stirred at high speed for 25 min to obtain a uniform emulsion pre-emulsion without stratification.

Emulsion polymerization

First, 15% water and 30% emulsifier were injected into a four-necked flask equipped with a nitrogen inlet and condensing reflux device, stirring at low speed with a magnetic force. When the temperature reached 80°C, 30% initiator solution and 20% pre-emulsion were added; at 0.5 h, a blue light appears in the emulsion polymerization when the seed emulsion begins to form. A peristaltic pump was used to slowly drop the residual pre-emulsion and initiator solution into a four-mouth flask to control the drop acceleration. After 4 h, the initiator solution and the pre-emulsion were discarded, the temperature was increased to 85°C, the insulation was held for 1 h, and then the material was filtered and discharged. A series of modified styrene-acrylic polymer emulsions were obtained by cooling the emulsion to room temperature, and the pH of the emulsion was adjusted to 7–8 by ammonia water.

Coating preparation

A transparent continuous coating was prepared by applying the appropriate amount of emulsion uniformly to the substrate by air spraying and air drying at room temperature for 24 h. Organic thermochromic materials were dispersed in silicone resin WB300 to prepare the coating. After 24 h of natural drying, a modified styrene-acrylic polymer emulsion with optimal weather resistance as the protective coating was sprayed onto the surface and allowed to dry naturally

at room temperature. Scheme 1 shows a diagram of the protective effect of the functional components of the coating surface on the UV light barrier and discoloration material.

Characterization

About 2 g of emulsion were applied evenly on clean aluminum foil, then baked at 100°C until the weight remained constant. Formulas (1) and (2) determined the solid content (S) and monomer conversion rate (C), respectively.

$$S(\mathrm{wt}\%) = \frac{W_2 - W_0}{W_1 - W_0} \times 100\% \tag{1}$$

$$C(\mathrm{wt}\%) = \frac{S \times W_3 - W_4}{W_5} \times 100\% \tag{2}$$

where W_0 represents the quality of aluminum foil, W_1 and W_2 represent the emulsion quality before and after drying. W_3 represents pre-polymerization input, W_4

Table 1: Emulsion polymerization formula

Component	Content/%						
	SA-0	SA-1	SA-2	SA-3	SA-4	SA-5	SA-6
MMA	13.3	11.4	11.1	10.8	10.6	10.3	10
St	5.2	4.5	4.4	4.3	4.1	4.0	3.9
BA	18.5	15.9	15.5	15.1	14.7	14.3	13.9
HEMA	2.0	2.0	2.0	2.0	2.0	2.0	2.0
AA	1.0	1.0	1.0	1.0	1.0	1.0	1.0
HFMA	0	3.0	3.0	3.0	3.0	3.0	3.0
VTMS	0	2.0	2.0	2.0	2.0	2.0	2.0
HMEB	0	0	0.8	1.6	2.4	3.2	4.0
EG	0.2	0.2	0.2	0.2	0.2	0.2	0.2
TX-100	1.0	1.0	1.0	1.0	1.0	1.0	1.0
SDBS	0.5	0.5	0.5	0.5	0.5	0.5	0.5
COPS-1	0.4	0.4	0.4	0.4	0.4	0.4	0.4
APS	0.3	0.3	0.3	0.3	0.4	0.3	0.3
$NaHCO_3$	0.3	0.3	0.3	0.3	0.5	0.3	0.3
DI-water	57.5	57.5	57.5	57.5	57.5	57.5	57.5

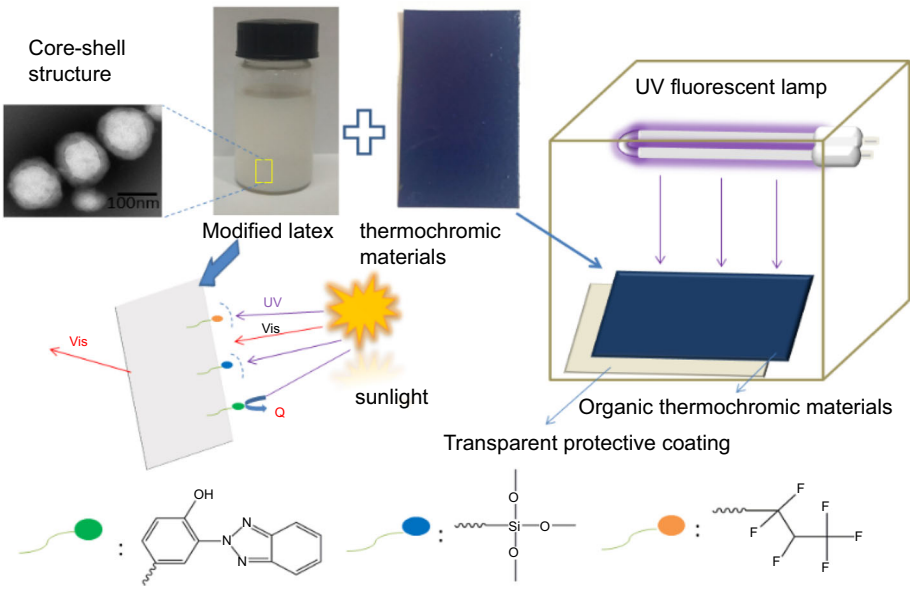

Scheme 1: Diagram of an application of UV absorption coating to weather resistance

represents a non-volatile group component, and W_5 represents a total monomer amount.

According to the GB/T 1733-1993 standard for coating water resistance, the coating was examined for bubbles and bleached after being immersed in water for 168 h. Formula (3) calculated the water absorption (δ):

$$\delta = \frac{W_6 - W_7}{W_6} \times 100\% \tag{3}$$

where W_6 represents the quality of the porous film, W_7 represents the quality of the dry film.

Seymour IS5 tested the infrared absorption spectrum. During the test, the emulsion coating with a thickness of about 20 μm was measured with a KBr sheet, the wavenumber range was set as 4000–400 cm^{-1}, the scanning number was 32, and the resolution was 4 cm^{-1}. TGA was performed on the STA449C synchronous thermal analyzer. The emulsion coating was dried at 80°C and made into powder. The addition rate was 10°C/min at 30°C to 700°C under argon gas. A UV-Vis 8500 tested spectrophotometer the UV absorption spectrum. The emulsion was uniformly applied to transparent glass sheets and dried at 80°C, and the wavelength range was set as 200–600 nm. The Malvern ZS90 instrument measured the nanoparticle size and zeta potential. The emulsion was diluted to a specific low concentration to test the particles' storage stability, size, and distribution in the emulsion.

The emulsion was diluted 1000 times with DI-water with ultrasonic vibration for 10 min. The emulsion was placed on a copper mesh and stained with tungsten phosphate. The morphology of different emulsion particles' sizes was observed under a transmission electron microscopy JM-1400Plus at an 80-120 kV voltage.

XPS was performed using the X-ray photoelectron spectrometer (Thermo Fisher Scientific K-Alpha) for the full and fine spectrum scanning of the membrane and air-surface elements. The latex film was prepared by drying at 80°C.

The coating weathering resistance test was performed in a GB/T 23987-2009 UV aging test chamber (China). During the test, the samples were cyclically exposed to UVB-313 radiation for 8 h and condensed for 4 h. The weathering resistance of polymer coatings was evaluated by the chromatic aberration (ΔE) and change in glossiness (ΔG). Three fixed positions on each sample surface were selected for testing. The color difference (ΔE) and light loss rate (ΔG) of the coatings were calculated by formulas (4) and (5), respectively.

$$\Delta E = \sqrt{\left(L_t^* - L_0^*\right)^2 + \left(a_t^* - a_0^*\right)^2 + \left(b_t^* - b_0^*\right)^2} \tag{4}$$

$$\Delta G = \frac{G_0 - G_t}{G_0} \times 100\% \tag{5}$$

where L^* stands for lightness, a^* (red-green-degree index), and b^* (yellow-blue-degree index) are chromaticity, and G stands for glossiness. Subscripts *0* and *t,* respectively, represent the parameter values before and after UV exposure for t hours.

Results and discussion

Basic properties of emulsions and the coatings

Table 2 shows the basic properties of the prepared emulsions and their coatings. The solid contents in the emulsions were around 41%, consistent with the theoretical values. The monomer conversion rate of SA-0 was the highest, reaching 97.3%. However, those of the emulsions SA-1∼SA-6 were around 94.5%. They had a slight decrease due to the incorporation of the modifying monomers, which had a steric hindrance effect on the polymerization of the monomers. All the emulsions existed in a homogenous fluid state after 1 year of storage without caking, showing good storage stability.

The SAC-0 water absorption rate was as high as 33.2%, while those values of the other coatings ranged from 3.3 to 7.9%, with no apparent difference among SAC-1 to SAC-6. This is due to the low polarity and excellent water resistance of organic fluorine and silicone. The water absorption of the coating increased slightly with the addition of HMEB, which may be due to the effect of large groups of HMEB on the crosslinking density of the coating. The chemically introduced fluorine and silicon monomers greatly improved the water resistance of coatings.

Zeta potential and DLS of emulsions

Zeta potential can evaluate the stability of the emulsion. When the zeta potential absolute value is greater than 30 mV, the stability is better. The zeta potentials and average particle size of various emulsions are shown in Fig. 1a. The zeta potentials of the emulsions are much higher than 30 mV because the anionic surfactants gave the emulsion particles a negative surface charge, indicating that the emulsions had good stability. With the continuous increase of functional monomers, the zeta potential of latex particles gradually shifted to a positive direction, and the stability declined; however, the absolute value remained higher than 30 mV.

The size and distribution of latex particles have an essential influence on the stability and film formation of the emulsion. Therefore, it is necessary to study the effect of different functional monomers on acrylate emulsion particle size. Figures 1a and 1b show that the latex particles size is mostly between 100 and 200 nm. The average particle size of SA-1 is much bigger than SA-0. This is because the fluorine and silicon mono-

Table 2: Basic properties of emulsions and the coatings

Emulsion	S (%)	C (%)	Storage stability	Coating	δ (%)	Water resistance
SA-0	41.8	97.3	stable	SAC-0	33.2	blistering
SA-1	41.0	95.4	stable	SAC-1	3.3	good
SA-2	40.8	94.8	stable	SAC-2	5.9	good
SA-3	40.7	94.6	stable	SAC-3	6.4	good
SA-4	40.5	94.1	stable	SAC-4	4.0	good
SA-5	41.0	95.4	stable	SAC-5	4.2	good
SA-6	40.9	95.1	stable	SAC-6	7.9	good

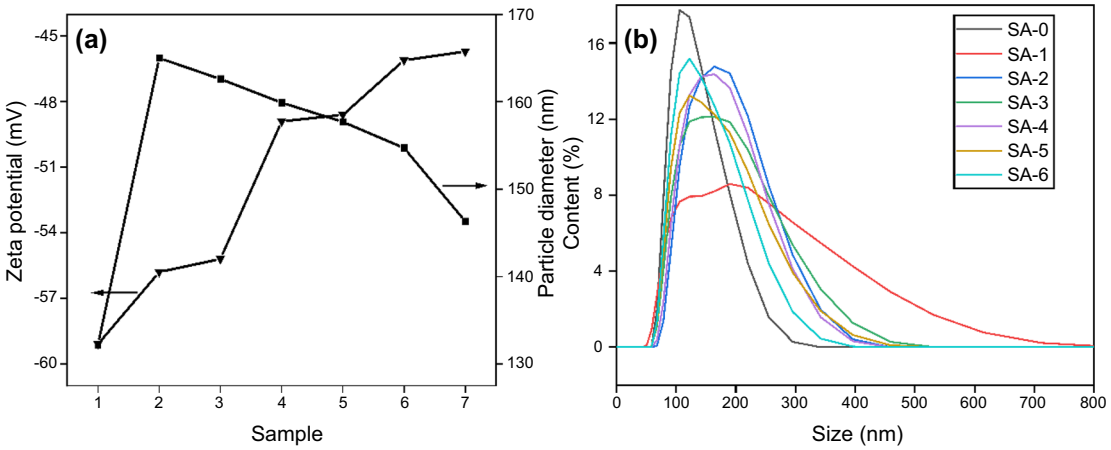

Fig. 1: Stability (zeta potential) of emulsion and average latex particle size (a) (sample 1: SA-0, sample 2: SA-1, sample 3: SA-2, sample 4: SA-3, sample 5: SA-4, sample 6: SA-5, sample 7: SA-6) and emulsion size distribution (b)

mers migrate to the surface of latex particles during copolymerization with other monomers, damaging the hydrophilic and oil-wet balance of latex particles, thus reducing the stability of latex particles and increasing the particle size of the emulsion. With HMEB content increase, the SA-2 to SA-6 particle size decreases linearly. It is possible that during HMEB polymerization, the large group site resistance hinders the adsorption of the emulsifier on the emulsion particles, increasing the number of emulsion particles, leading to a decrease in the average size of the particles, and the reduction of emulsion potential with the rise of HMEB.

Morphology of emulsion particles

The micromorphology of emulsion particles was characterized by TEM, and the results are shown in Fig. 2. The latex particles show a uniform size and a spherical shape. The SA-1 latex particle size varies significantly from 100 to 500 nm, consistent with the DLS results. The result indicates that a target emulsion with good fluidity and uniform particle size has been successfully prepared.

Chemical structure of emulsion polymer

Infrared spectroscopy is used to characterize the group structure of organic coatings and compare the variation on the absorption peaks of different coatings. All coatings show the C–H stretching vibration peaks of $–CH_3$ and $–CH_2–$ and the bending vibration absorption peak of $–CH_3$ at 2957, 2867 and 1382 cm^{-1}, respectively (Fig. 3). The stretching vibration absorption peaks of C=O and C–O–C in the ester group appear at 1730 cm^{-1} and 1162 cm^{-1}. The skeleton vibration absorption peak of the benzene ring appears at 1455 cm^{-1}, and the vibration absorption peak of the C–H of the benzene ring appears at 764 cm^{-1} and 702 cm^{-1}. Compared to SAC-0, SAC-1 has a weak C–F absorption peak at 1238 cm^{-1}, and because of the overlapping peaks of C–F, Si–O, and C–O, the absorption band from 1000 to 1240 cm^{-1} in the spectrum of SAC-1 becomes significantly broader and stronger, indicating that the fluorine and silicon monomers have been incorporated in the coatings.[7] The SAC-5 spectra show new characteristic peaks at 1600 cm^{-1} and 1341 cm^{-1} attributed to the vibration absorption peak of benzotriazole ring skeleton and the stretching vibration peak of C–N in the UV absorption monomer, respectively, indicating the suc-

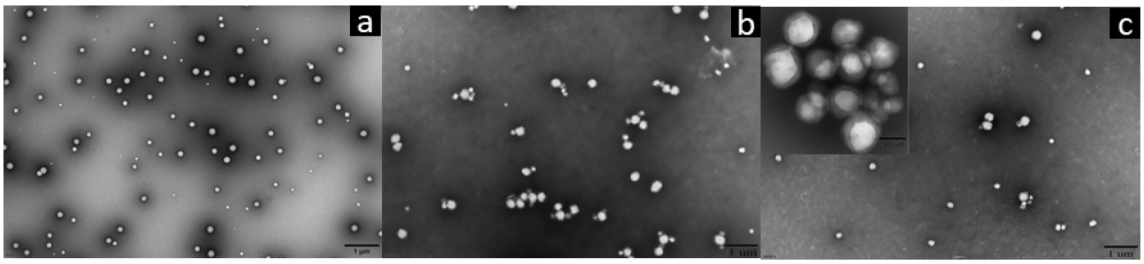

Fig. 2: TEM imaging of SA-0 (a), SA-1 (b) and SA-5 (c) emulsion particles

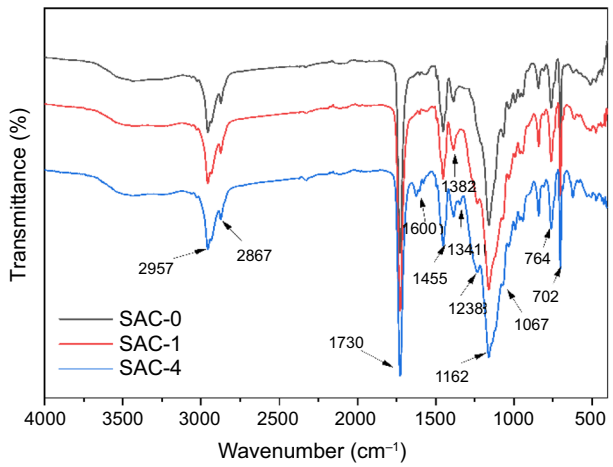

Fig. 3: FTIR of different emulsion coatings

cessful preparation of UV-absorbing fluorine- silicon acrylate emulsion.

Chemical composition of emulsion coatings

XPS analyzed the surface chemical composition of emulsion coatings because each element has its unique binding energy. As shown in Fig. 4a, SAC-0 has three peaks, C 1s, O 1s, and Na 1s, appearing at 285 eV, 531 eV, and 1072 eV, respectively. After modification by fluorine and silicon monomers, the spectra of SAC-1 show new peaks at 100 eV, 150 eV, and 685 eV, corresponding to Si 2s, Si 2p, and F 1s, respectively. SAC-4 was modified by the benzotriazole UV absorber, so the N 1s peak appears at 398 eV. Figures 4b–4d show the fitting separation of C 1s spectra of SAC-0, SAC-1, and SAC-4 by the Avantage software. The three peaks of SAC-0, SAC-1, and SAC-4 were designated as C–C, C–O, and C=O, respectively, at 284.8 eV, 286.2 eV, and 288.6 eV. After SAC-1 and SAC-4 modification, the peaks of C-Si, C–F, and $-CF_3$ also appear at 283.2 eV, 287.2 eV, and 292.8 eV. Compared with SAC-1, the C–F peak was slightly increased and the C–Si peak was significantly decreased, indicating that the functional monomers, including UV absorbers, fluorine, and silicon monomers, were successfully introduced into the coating. The peak area changes of C–Si and C–F were consistent with the results in Table 3. As shown in Table 3, with the addition of HMEB, the F element range on the coating surface increases from 0.71 to 1.01%, while the Si element content decreased from 2.86 to 1.48%. In theory, the N element content is only 0.73% and increased to 1.45%, indicating that the UV-absorbing monomer tends to concentrate on the coating surface. This suggests that the silicon crosslinking reaction on the surface of the film is delayed by the large group structure of HMEB, promoting the migration of fluorine to the coating surface.

UV absorption property of coatings

The emulsion coatings were tested by UV-Vis transmission spectrum with the wavelength ranged from 200 to 600 nm, as shown in Fig. 5. SAC-0 has a good light transmittance; however, the value of SAC-1 modified with fluorine and silicon monomers was significantly reduced in the UV region. This is mainly due to the fluorine and silicon elements specific shielding effect of UV lights. By introducing UV absorbers, the light transmittance of the coatings begins to decrease significantly at 258 nm, and that value drops to 0% in the range from 308 to 364 nm, showing a complete UV barrier. Interestingly, the coatings show a wider complete barrier range to the UV region with the UV absorber increases. This has potential applications in protecting organic thermochromism material, which requires good transmittance in the visible region and good shielding performance in the UV region.

As shown in Fig. 6, HMEB contains a conjugated electron structure and proton transfer structure. After absorbing UV light, the excited hydroxyl group forms an internal hydrogen bond chelating ring with the adjacent nitrogen atom. The two UV absorption peaks are formed by the transition of the outer layer π electrons in an excited state to an anti-bonding empty orbital π^*.[28,32] The tautomer formed by proton transfer are unstable and will release the excess energy in the form of heat energy to form a stable structure. The above results showed that HMEB was incorporated successfully in the polymer emulsion, and the coating has a UV absorption function.

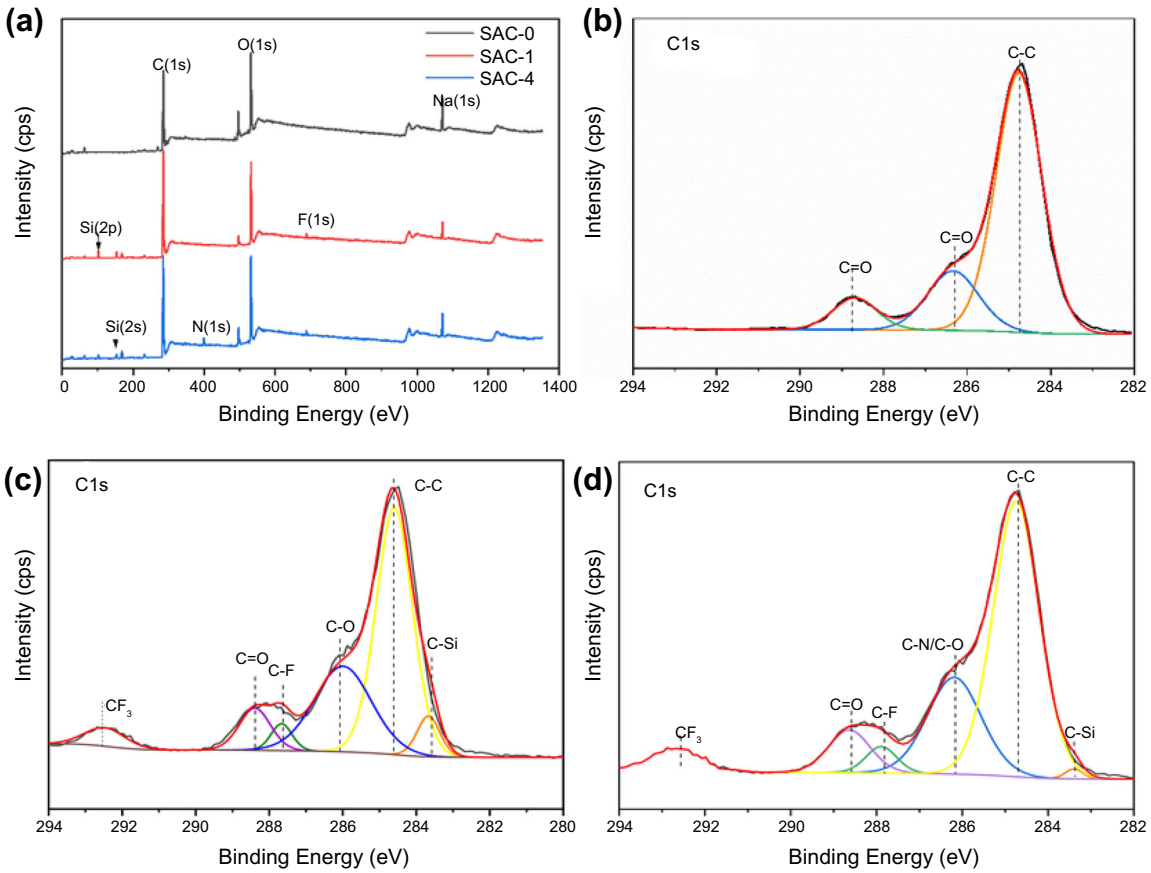

Fig. 4: XPS full spectrum of SAC-0, SAC-1 and SAC-4 with different transparent coatings formulations (a), high-resolution C 1s spectrum of SAC-0 coating (b), SAC-1 coating (c) and SAC-4 coating (d)

Table 3: Surface composition of different coatings/ atomic %

Coating	C	O	F	Si	N
SAC-0	69.11	30.89	–	–	–
SAC-1	69.63	26.8	0.71	2.86	–
SAC-4	72.57	23.49	1.01	1.48	1.45

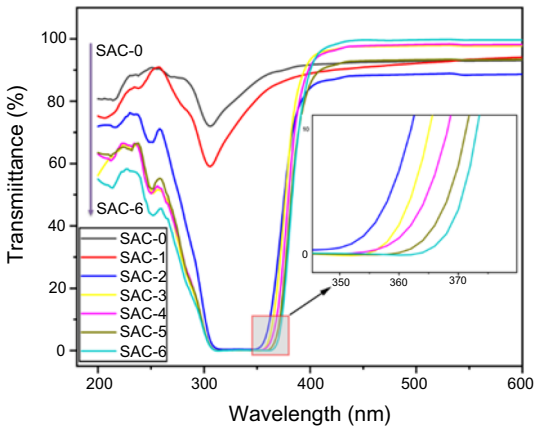

Fig. 5: UV-Vis transparent spectra of different transparent coatings formulations

Thermal stability of emulsion coatings

To study the influence of functional monomers on the thermal stability of polymer coatings, the results of TGA characterization are shown in Fig. 7. All coatings have only one thermal decomposition process and no significant weight change before 300°C. SAC-0 begins to lose weight rapidly at 327°C. In contrast, the other coatings start to lose weight at 339°C because of the modification of fluorine and silicone monomers. This can be explained that C–F and Si–O with high bond energies form a shielding protection effect on the C–C main chain, thus improving the thermal stability of polymer coating.[31] The addition of HMEB has a low impact on the thermal stability of the coating, and the thermal decomposition curves of SAC-1 and SAC-5 are the same. When the temperature reaches 500°C, the quality of all coatings no longer changes.

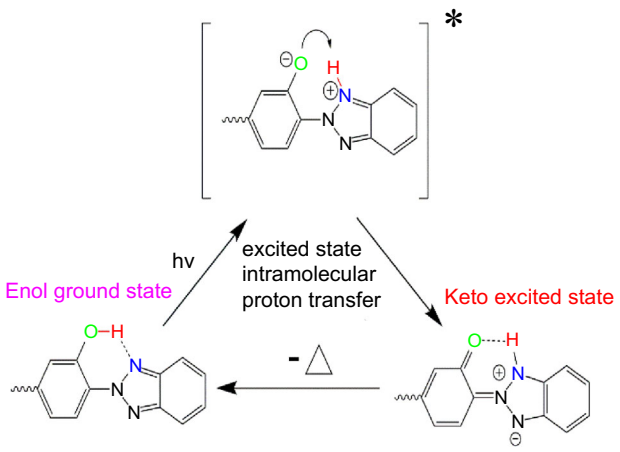

Fig. 6: Absorption mechanism diagram of UV absorption coating

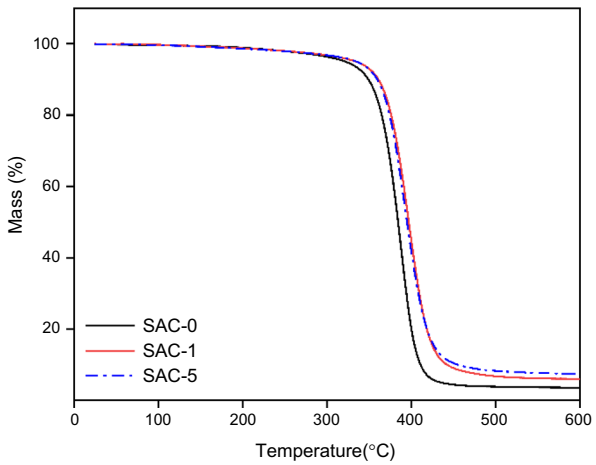

Fig. 7: TGA of different transparent coatings formulations

The aging acceleration test of emulsion coatings

As shown in Fig. 8, SAC-0 has the greatest sensitivity to UV aging. After 200 h of accelerated aging, the ΔG reaches 26.59%, and the change rate of light loss rate is the largest among all coatings. After 800 h, the ΔG reaches 73.11% and then tends to a balance. Compared with SAC-0, the ΔG of SAC-1 is only 17.46% after 200 h accelerated aging and 72.22% after 1000 h aging. After modification by fluorine and silicon monomers, the UV-durability was enhanced because of Si–O and C–F, which are difficult to degrade by UV due to their high bond energies. After 200 h accelerated aging, the ΔG values of coatings from SAC-2 to SAC-6 are controlled between 3.91 and 7.94%. Even after 1000 h accelerated aging, the ΔG of SAC-6 is 51.10%, far lower than SAC-0. Coatings modified by UV absorbers have UV shielding properties, which reduce the intensity of UV light and thus reduce damage. Moreover, this property is increased with the amount of UV absorber introduced in the coating.

The ΔE with aging time is one of the essential references to the anti-aging ability of coatings. As shown in Fig. 9, the delta ΔE of all coatings shows rapid growth followed by slow growth. SAC-0 and SAC-1 modified by fluorine and silicon monomers are significantly yellowed after 200 h of accelerated aging, with the former showing a significant yellow color change. After 1000 h UV aging, the ΔE of SAC-0 is 16.05, and that of SAC-6 is reduced to 6.86, and the ΔE of other coatings is between these two and decreases with the content of reacted UV absorbers, indicating that the incorporated UV absorbers can significantly improve the UV resistance. Moreover, the fluorine and silicon monomers also promote the modified weatherability. Based on the synergetic results, the weatherability of coatings reaches new heights.

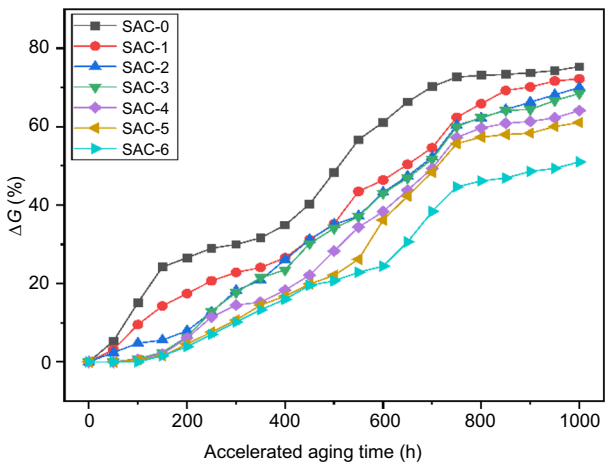

Fig. 8: ΔG of UV aging of 1000 h with different transparent coatings formulations

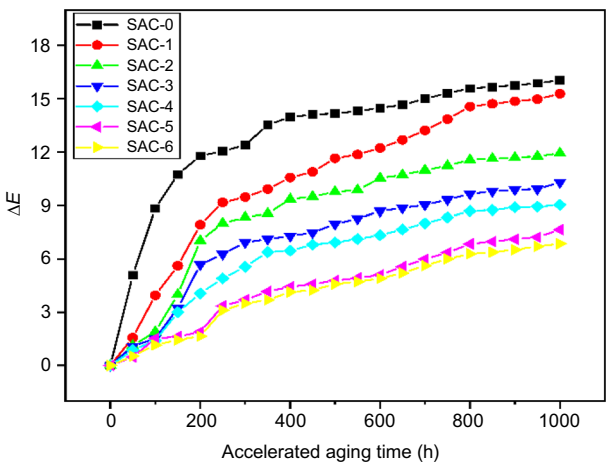

Fig. 9: ΔE of UV aging for 1000 h with different transparent coatings formulations

Protective properties of emulsion coatings

Organic thermochromic materials are temperature indicators, so they have potential applications in industrial, medical, and textile fields. Given the poor UV-durability of commercially available organic thermochromic material (blue–white), new thermochromic material was prepared on tinplate with silicone WB300 as a binder and self-made emulsion a protective layer in this paper.

The change of b* value (yellow–blue degree index) was taken as a reference value. The more negative b* is, the bluer it is, and the more positive b* is, the yellower. As shown in Fig. 10, the b* of blank thermochromic material indicates linear change at the beginning, then tends to balance with a final Δb* of 4.28. In addition, cracking of the coating can be seen after 56 h of UV exposure. After 56 h UV irradiation, the Δb* of the thermochromic material with SAC-0 as the protective coating is 8.05. This is because SAC-0 itself contains color-changing groups. Compared with SAC-1, Δb* of the material with SAC-2 as the protective layer is reduced to 4.08. The introduced fluorine and silicon monomers have a protective shielding effect on the coatings. However, the protective ability is still not ideal, and bubbles appear on the surface after 56 h UV radiation. SAC-6 has the best protection for organic thermochromic material. After 100 h UV irradiation, Δb* of the organic thermochromic coating is only 0.84 and consistent with primary colors. Also, the protection provided by UV absorption coatings can be extended from organic thermochromic materials to most organic dyes used in coatings for better outdoor conditions.

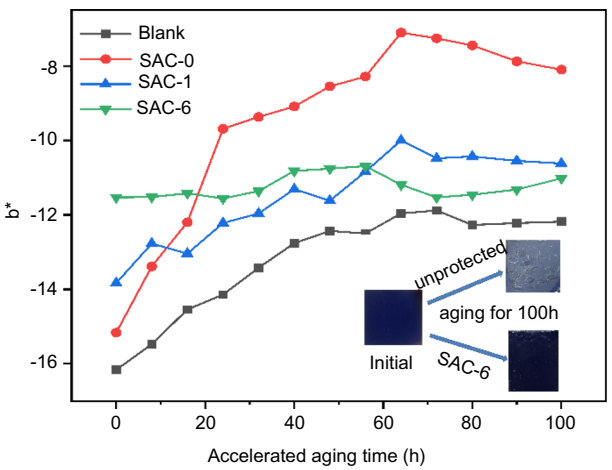

Fig. 10: Changes of b* after UV accelerated aging of thermochromic materials with different transparent coatings formulations for 100 h

Conclusions

In this study, a series of modified styrene-acrylic emulsions with UV-absorbing ability were successfully prepared by emulsion polymerization. Copolymers containing a combination of 2% VTMS, 3% HFMA, and 4% HMEB have the best weathering properties in styrene-acrylic coatings. Based on the UV absorption spectra, the coatings showed a complete UV barrier from 308 to 364 nm and greater intensity of the UV barrier with increasing HMEB. Compared to the unmodified coating, the water absorption rate decreased from 33.2 to 4%, while the initial decomposition temperature increased from 327 to 339°C. Altogether, the water resistance and thermal stability of the modified coatings were improved.

Introduced UV absorbers improved the weatherability of the coating. After 1000 h UV accelerated aging, the (ΔE) and (ΔG) of the coating were 6.86 and 51.0%, while those of the unmodified coating were as high as 16.05 and 73.11%, respectively. Moreover, the Δb* of the thermochromic material with the new protective coating was only 0.84 after UV aging of 100 h. This new UV-durability emulsion has excellent potential in protective coatings with high requirements for outdoor weather resistance.

Acknowledgments The authors are grateful for the support of Huibin Lei in the course of the presented research work and characterization technique. This research did not receive any specific grant from funding agencies in the public, commercial, or not-for-profit sectors.

Data availability The raw/processed data required to reproduce these findings cannot be shared at this time due to technical or time limitations.

Conflict of interest The authors declare that they have no known competing financial interests or personal relationships that could have appeared to influence the work reported in this paper.

References

1. Machotova, J, Cernoskova, E, Honzicek, J, Snuparek, J, "Water sensitivity of fluorine-containing polyacrylate latex coatings: Effects of crosslinking and ambient drying conditions." *Prog. Org. Coat.*, **120** 266–273 (2018)
2. Huang, K, Liu, Y, Wu, D, "Synthesis and characterization of polyacrylate modified by polysiloxane latexes and films." *Prog. Org. Coat.*, **11** 1774–1779 (2014)
3. Zheng, B, Ge, S, Wang, S, Shao, Q, Jiao, C, Liu, M, Das, R, Dong, B, Guo, Z, "Effect of γ-aminopropyltriethoxysilane on the properties of cellulose acetate butyrate modified acrylic waterborne coatings." *React. Funct. Polym.*, **148** 104484 (2020)

4. Kotlík, P, Doubravova, K, Horalek, J, Lubomír, K, Jiri, A, ''Acrylic copolymer coatings for protection against UV rays.'' *J. Cult. Herit.*, **15** 44–48 (2014)
5. Lei, H, He, D, Guo, Y, Tang, Y, Hou, H, ''Synthesis and characterization of UV-absorbing fluorine-silicone acrylic resin polymer.'' *Appl. Surf. Sci.*, **442** 71–77 (2018)
6. He, S, Liu, W, Yang, M, Liu, C, Jiang, C, Wang, Z, ''Fluorinated polyacrylates containing amino side chains for the surface modification of waterborne epoxy resin.'' *J. Appl. Polym. Sci.*, **136** 47091 (2019)
7. Lu, T, Qi, D, Zhang, D, Liu, Q, Zhao, H, ''Fabrication of self-cross-linking fluorinated polyacrylate latex particles with core-shell structure and film properties.'' *React. Funct. Polym.*, **104** 9–14 (2016)
8. Bader, T, Lackner, R, ''Acrylic surface treatment applied to architectural High-Performance Concrete (HPC): Identification of potential pitfalls on the way to long-lasting protection.'' *Constr. Build. Mater*., **237** 117415 (2020)
9. Liu, F, Liu, G, ''Enhancement of UV-aging resistance of UV-curable polyurethane acrylate coatings via incorporation of hindered amine light stabilizers-functionalized TiO_2-SiO_2 nanoparticles.'' *J. Polym. Res.*, **25** 59–72 (2018)
10. Li, N, Bao, M, Rao, F, Shu, Y, Huang, C, Huang, Z, Chen, Y, Bao, Y, Guo, R, Xiu, C, ''Improvement of surface photostability of bamboo scrimber by application of organic UV absorber coatings.'' *J. Wood Sci.*, **65** 7–15 (2019)
11. Dong, L, Liu, X, Xiong, Z, Sheng, D, Lin, C, Zhou, Y, Yang, Y, ''Preparation and characterization of functional poly(vinylidene fluoride) (PVDF) membranes with ultraviolet-absorbing property.'' *Appl. Surf. Sci.*, **444** 497–504 (2018)
12. Nguyen, T, Nguyen, TP, Azizi, S, ''The role of organic and inorganic UV-absorbents on photopolymerization and mechanical properties of acrylate-urethane coating.'' *Mater. Today Commun*., **22** 100780 (2020)
13. Lei, H, He, D, Hu, J, Li, P, Huang, H, ''Modification of a fluorine-silicone acrylic resin with a free-radical-catching agent.'' *J. Coat. Technol. Res.*, **15** 809–817 (2018)
14. Dhineshbabu, NR, Bose, S, ''Smart textiles coated with eco-friendly UV-blocking nanoparticles derived from natural resources.'' *ACS Omega*, **3** 7454–7465 (2018)
15. Martín-Fabiani, I, Koh, ML, Dalmas, F, ''Design of waterborne nanoceria/polymer nanocomposite UV-absorbing coatings: Pickering versus blended particles.'' *ACS Appl. Mater. Inter.*, **1** 3956–3968 (2018)
16. Álvarez-Asencio, R, Corkery, RW, Ahniyaz, A, ''Solventless synthesis of cerium oxide nanoparticles and their application in UV protective clear coatings.'' *RSC Adv.*, **10** 14818–21482 (2020)
17. Peng, L, Lin, M, Zhang, S, Li, L, Fu, Q, Hou, J, ''A self-healing coating with UV-shielding property.'' *Coatings*, **9** 423-435 (2019)
18. Rao, F, Zhang, Y, Bao, M, ''Photostabilizing efficiency of acrylic-based bamboo exterior coatings combining benzotriazole and zinc oxide nanoparticles.'' *Coatings*, **9** (9) 533–541 (2019)
19. Yang, M, Liu, W, Jiang, C, Xie, Y, Shi, H, Zhang, F, Wang, Z, ''Facile construction of robust superhydrophobic cotton textiles for effective UV protection, self-cleaning and oil-water separation.'' *Colloids Surf. A*, **570** 172–181 (2019)
20. Ren, G, Song, Y, Li, X, Wang, B, Zhou, Y, Wang, Y, Ge, B, Zhu, X, ''A simple way to an ultra-robust superhydrophobic fabric with mechanical stability UV durability, and UV shielding property.'' *J. Colloid Interface Sci.*, **522** 57–62 (2018)
21. Zhu, T, Li, S, Huang, J, ''Rational design of multi-layered superhydrophobic coating on cotton fabrics for UV shielding, self-cleaning and oil-water separation.'' *Mater. Des.*, **134** 342–351 (2017)
22. Li, S, Huang, J, Chen, Z, Chen, G, Lai, Y, ''A review on special wettability textiles: Theoretical models, fabrication technologies and multifunctional applications.'' *J. Mater. Chem. A*, **5** 31–55 (2017)
23. Dong, X, Gao, S, Huang, J, ''A self-roughened and biodegradable superhydrophobic coating with UV shielding, solar-induced self-healing and versatile oil–water separation ability.'' *J. Mater. Chem. A*, **7** 2122–2128 (2019)
24. Grigsby, W, Steward, D, ''Applying the protective role of condensed tannins to acrylic-based surface coatings exposed to accelerated weathering.'' *J. Polym. Environ.*, **26** 895–905 (2017)
25. Grigsby, WJ, ''Photooxidative stability provided by condensed tannin additives in acrylic-based surface coatings on exterior exposure.'' *J. Coat. Technol. Res.*, **15** 1273–1282 (2018)
26. González, MTP, Fumagalli, F, Benevenuto, CG, ''Novel benzophenone-3 derivatives with promising potential as UV filters: Relationship between structure, photoprotective potential and phototoxicity.'' *Eur. J. Pharm. Sci.*, **101** 200–210 (2017)
27. Agnieszka, GK, Karolina, S, Justyna, P, ''Cinnamic acid derivatives in cosmetics current use and future prospects.'' *Int. J. Cosmet. Sci.*, **40** (4) 356–366 (2018)
28. Lei, H, He, D, Hu, J, ''A fluorine–silicone acrylic resin modified with UV-absorbing monomers and a free radical scavenger.'' *J. Coat. Technol. Res.*, **15** (4) 809–817 (2018)
29. Wu, Y, Zhu, C, Yanchen, Z, Qiu, H, Ma, H, Gao, C, ''A type of silicone modified styrene-acrylate latex for weatherable coatings with improved mechanical strength and anticorrosive properties.'' *React. Funct. Polym*., **148** 104484 (2020)
30. Kook, JW, Kim, Y, Hwang, K, Kim, J, Lee, JY, ''Synthesis of poly(methyl methacrylate-co-butyl acrylate)/perfluorosilyl methacrylate core-shell nanoparticles: Novel approach for optimization of coating process.'' *Polymers*, **10** 1186–1198 (2018)
31. Hao, G, Zhu, L, Yang, W, Chen, Y, ''Investigation on the film surface and bulk properties of fluorine and silicon contained polyacrylate.'' *Prog. Org. Coat.*, **85** 8–14 (2015)
32. Naumov, S, Herzog, B, Abel, B, ''Spectra and photorelaxation of hydroxyphenyl-benzotriazole-type UV absorbers: From monomers to nanoparticles.'' *J. Phys. Chem. A*, **124** 625–632 (2020)